OPTIMAL DESIGN OF THERMO-OPTIC DEVICES ON THE SILICON-ON-INSULATOR PLATFORM

LE TRUNG THANH

ABSTRACT

A novel design of devices based on the thermo-optic effect in silicon on insulator (SOI) waveguides is presented. In order to evaluate accurately the temperature distribution and speed of the device, the heat transfer equation is to be solved numerically. It will be shown in this paper how the new thermo-optic waveguide structure, in which air trenches are made, can improve the performance of the thermo-optic device. In addition, a new formula for calculating the phase shift induced by the thermo-optic effect is proposed.

Keyword. Thermo-optic effect, silicon on insulator, optical devices

1. INTRODUCTION

In recent years, silicon on insulator (SOI) technology has been used for the design and implementation of various integrated-optic devices. It is because the fabrication of such devices requires only small and low cost modifications to existing fabrication processes. SOI technology is compatible with existing complementary metal–oxide–semiconductor (CMOS) technologies for making compact, highly integrated and multifunction devices [1]. The SOI platform uses silicon both as the substrate and the guiding core material. The large index contrast between Si (n_{Si} = 3.45 at wavelength 1550 nm) and SiO_2 (n_{SiO_2} = 1.46) allows light to be confined within submicron dimensions and single mode waveguides can have core cross-sections with dimensions of only few hundred nanometers and bend radii of a few micrometers with minimal losses. Moreover, SOI technology offers potential for monolithic integration of electronic and photonic devices on a single substrate. A variety of photonic devices have been designed and realized on the SOI platform, including lasers [2], high speed optical modulators [3] and optical switches [4].

Active devices on the SOI platform such as optical switches, filters and modulators rely on either the free carrier- or thermo-optic effect. A new design for thermo-optic waveguides on the SOI platform is presented in this paper. In addition, for the first time, an accurate calculation of the phase shift induced by the thermo-optic effect is proposed. Silicon has a very high thermo-optic coefficient, allowing fairly low transmission loss, low cost, high stability, low power consumption, fast response time and very large scale integration. Our new design can be used for active optical devices using the thermo-optic effect on the SOI platform such as optical switches

and optical filters based on Mach- Zehnder Interferometer (MZI) and microresonator structures [5].

2. OPTIMAL DESIGN FOR SOI THERMO-OPTIC WAVEGUIDES

Consider two alternative cross-sections for a heated waveguide as shown in Fig. 1(a) and 2(b), respectively. The upper cladding thickness t_{SiO_2} between the heater and the top of the rib must be thick enough to insulate the waveguide core from the metallic electrode and to reduce attenuation of the light by their field interaction. In all designs, Aluminum (Al) is used as the heater electrode. The thickness of the heater is $t_H = 0.5$ μm. At an operating wavelength of $\lambda = 1550$ nm, the refractive index of Al is $n_{Al} = 1.44 - j16$ [6]. The loss due to the presence of the metal electrode calculated using the FEM method is about 0.012 dB/cm at a thickness of $t_{SiO_2} = 0.5$ μm. Therefore, a thickness of 0.5μm is used in these designs. The under cladding thickness is $h_{SiO_2} = 1.3$ μm.

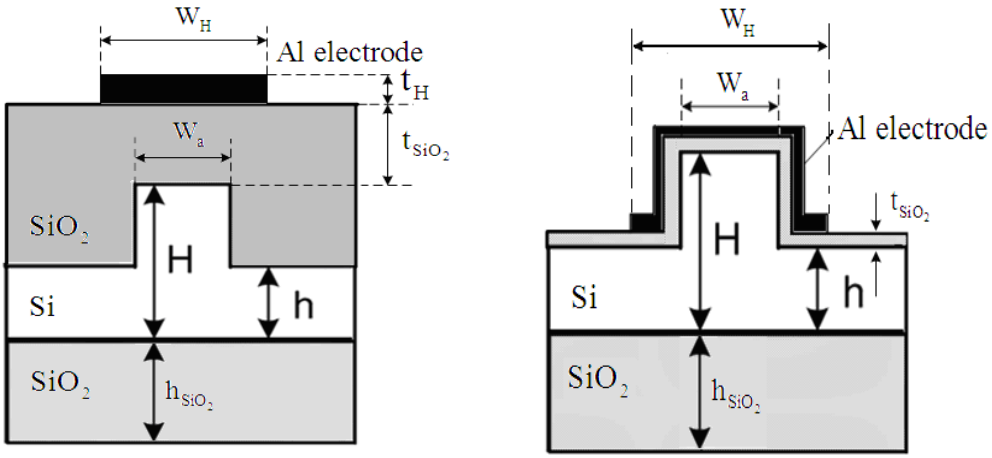

Figure 1. Two conventional structures for the heated waveguides

The heat transfer equation in each material layer can be expressed by [7]

$$\rho_m C_m \frac{\partial T}{\partial t} = k_m \nabla^2 T + Q(x, y, z, t) \tag{1}$$

where ρ_m, C_m and k_m are the thermal density, specific heat capacity and thermal conductivity of the material, respectively. Q(x,y,z,t) is the heat generation rate per unit volume. T is the temperature distribution across the guide in each layer and t is time.

Since the thermal conductivity of silicon is high, the silicon substrate is used as a heat sink with an initial condition $T(x, y, z, t)\big|_{t=0} = 25^0 C$. It is assumed that the analyzed domain is large

enough so that there is negligible heat transfer across the left and right hand-side boundaries. The boundary conditions become

$$-\frac{\partial T}{\partial \hat{\mathbf{n}}} = \delta(T_s - T_a) \text{ on the top surface} \tag{2}$$

$$-\rho\frac{\partial T}{\partial \hat{\mathbf{n}}} = 0 \text{ on the lateral surface} \tag{3}$$

where $\hat{\mathbf{n}}$ is the surface outward normal, δ is the natural heat transfer coefficient, T_s is the surface temperature and T_a is the air temperature.

It will be shown that the lateral spreading of the heat in these conventional design is large. This results in a large transverse separation required to thermally isolate the thermo-optic waveguide from any adjacent waveguides. In order to obtain good thermal isolation between the two thermo-optic waveguides and to improve the efficiency of heat transfer to the waveguide core, a modified design is proposed. This design incorporates air trenches etched into the silicon waveguide core remote from the core region.

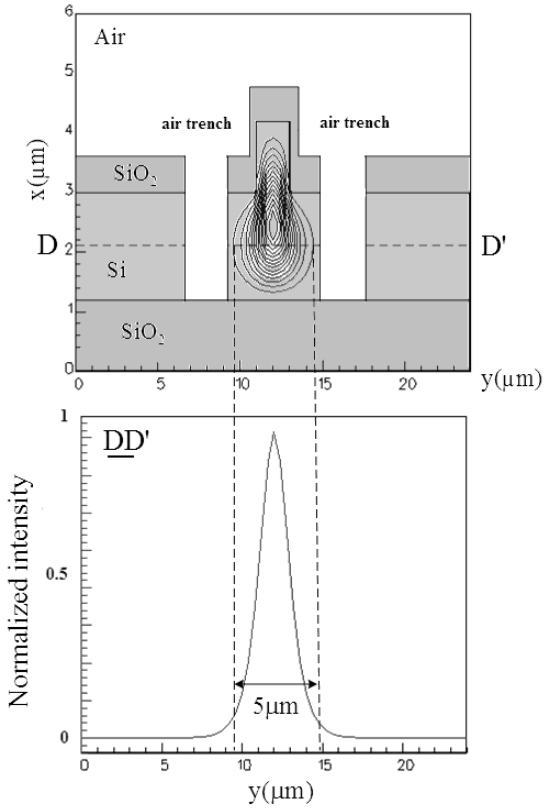

Figure 2. A modified design for the thermo-optic waveguide incorporating the air trenches. The air trenches are determined by the field profile in the waveguide core (the line DD')

Consider the modified heated waveguide structure presented in Fig. 2, which incorporates two air trenches having a depth of $2.3\ \mu m$. The optical waveguide has a rib height H = 3 μm, lateral slab height h = 1.8 μm and waveguide width $W_a = 2$ μm. It is desired to locate the air trenches as near to the waveguide core as possible. This enables better performance of the thermo-optic device to be achieved. To determine the positions of the air trenches, the power field profile in the waveguide is used. From Fig. 2, the width of the field at which the field becomes negligible is about 5 μm. The best positions for the air trenches are also shown in Fig. 2.

3. SIMULATIONS AND DISCUSSIONS

In this section, the FEM is used to evaluate the performance of the proposed structure and to compare its performance to the conventional designs. Since the length L_H of the heater is much longer than its width W_H, a two dimensional analysis can be used. The following values of thermal conductivity, density and specific heat capacity are used in the simulations: $k_{Si} =$ 163 W/mK, $C_{Si} =$ 0.703 J/gK, $\rho_{Si} =$ 2.330 g/cm^3, for silicon, and $k_{air} = 0.026$ W/mK, $\rho_{air} = 1.166.x10^{-3}\, g/cm^3$, $C_{air} = 1.005\ J/g.K$ for air layers, respectively. A heater width of 5 μm is used in all the simulations.

One important parameter, which has an important effect on device performance, is the lateral (heat) spreading coefficient. In the designs, this value needs to be taken into account. In this paper, the lateral spread length can be calculated accurately by the 2D FEM.

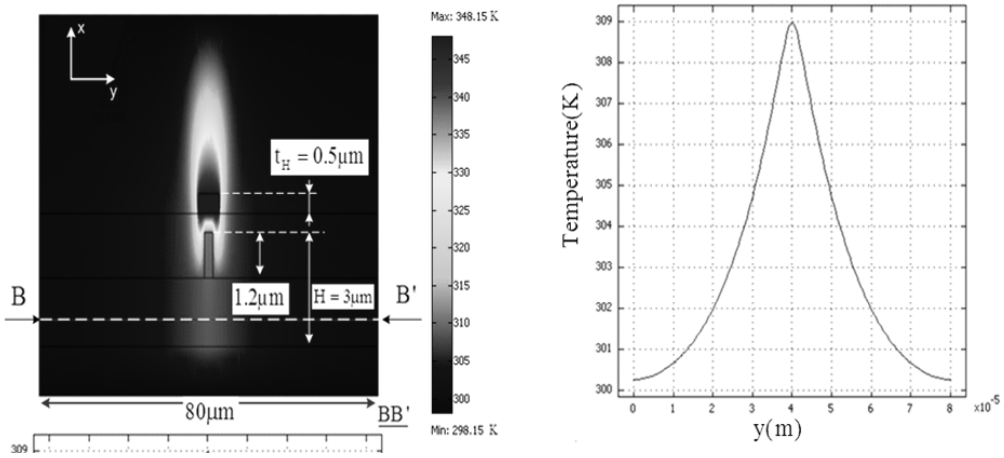

Figure 3. Typical temperature distribution and horizontal profile along the section BB' of the waveguide shown in Fig. 1(a) for the heater temperature of 75°C

Figure 3 shows a typical thermal distribution across the waveguide of Fig. 1(a) for a heater temperature of 75^0C (or 348 K). The temperature profile along the line BB' is also shown. The thermal distribution (for the same heater temperature) for the waveguide structure in Fig. 1(b) is plotted in Fig. 4. The thermal spread width ΔW_{th} calculated from this simulation is about

20 μm for both cases. However, it is obvious from the simulations that the second thermo-optic waveguide structure (Fig. 1(b)) is more effective than the first case. At the same heater temperature, more heat is transferred to the core waveguide in the second case.

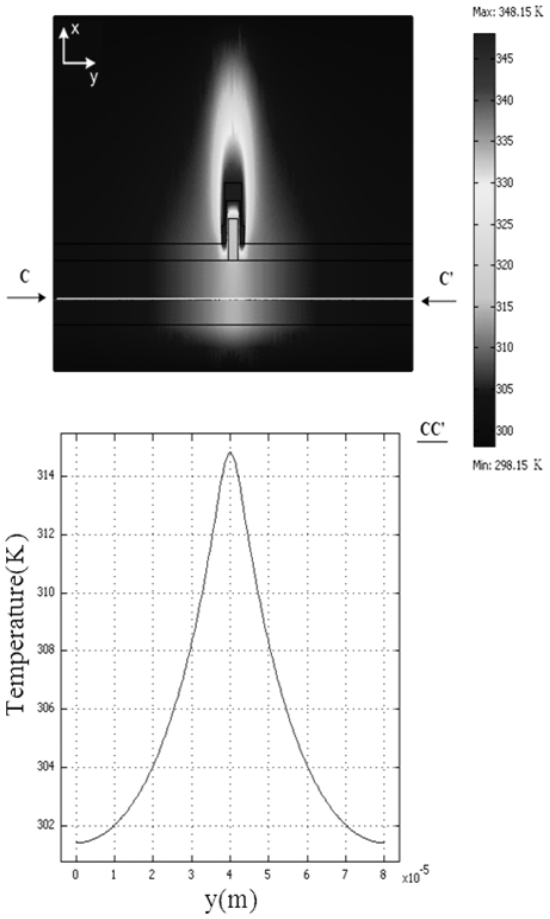

Figure 4. Temperature distribution and horizontal profile along the section CC' of waveguide shown in Fig. 1(b) at the heater temperature of 75°C

The heat distribution in the case of the thermo-optic waveguide having air trenches with a width of 5 μm is shown in Fig. 5(a). Figure 5(b) shows the horizontal temperature profile at the centre of the waveguide. It is clear that the lateral heat spreading is reduced significantly. In addition, more heat is transferred into the core waveguide. This result enables the heater power consumption to be reduced.

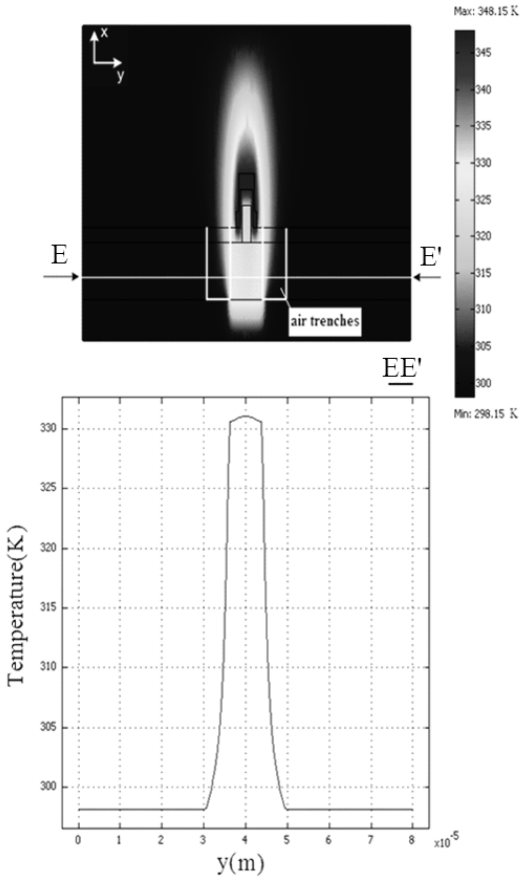

Figure 5. Temperature distribution and horizontal profile along the line EE' of the waveguide for the modified design in Fig. 4.45 at the heater temperature of 75°C

By increasing the heater temperature in 50°C steps from 25°C to 425°C in the simulations, the relevant temperature distribution in every waveguide layer can be determined as a function of heater temperature. The refractive index change is then calculated for each layer of the structure and for each temperature by using the bulk thermo-optic coefficients $(\frac{\partial n}{\partial T})\Big|_{Si} = +1.86x10^{-4}/K$ for silicon and $(\frac{\partial n}{\partial T})\Big|_{SiO_2} = +1x10^{-5}/K$ for silica. These new refractive indices are then used as input variables for the modal analysis. As a result, new effective indices n_e and the effective thermo-optic coefficient $\frac{\partial n_e}{\partial T}$ are finally derived. Figure 4.47 shows the calculated effective refractive index change Δn_e versus the heater temperature change ΔT in the structures shown in Fig. 1 and Fig. 2.

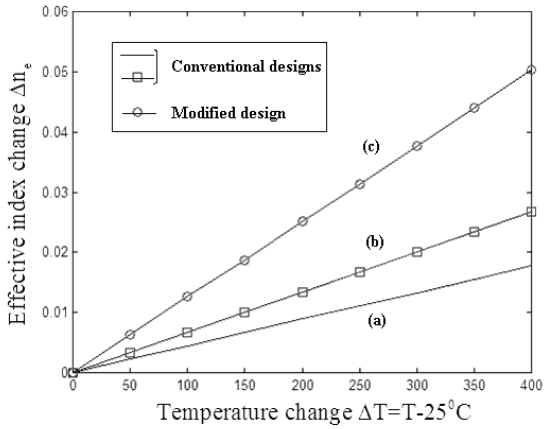

Figure 6. Effective refractive index change versus heater temperature change for three designs (a) the design shown in Fig. 1(a) (b) the design shown in Fig. 1(b) and (c) the new design having two air trenches shown in Fig. 2

A change in effective refractive index will introduce a phase shift. In the literature, the length of the heater is often its actual length and the phase shift can be calculated by

$$\Delta\varphi = \frac{2\pi}{\lambda}\Delta n_e L_H . \tag{4}$$

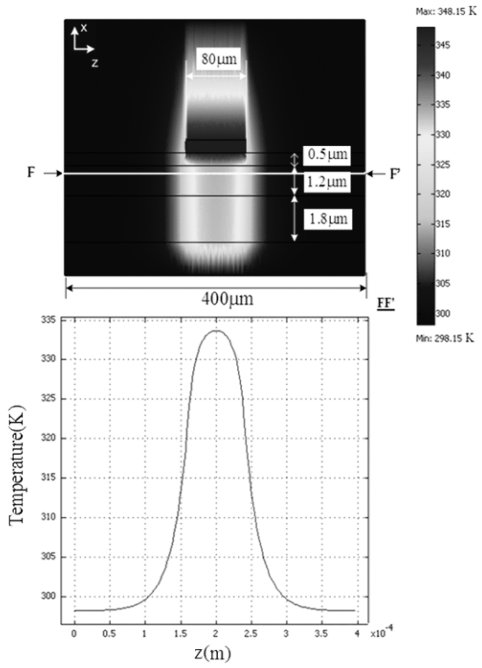

Figure 7. The temperature distribution $T_e(z)$ along the propagation direction and temperature profile along the section FF' of the waveguide core

However, in order to accurately determine the heated length, the length of the heater should include the actual length L_H and the thermal spreading length ΔL_{pth} along the propagation direction. To calculate this thermal spreading length, the 2D-FEM is used. A 2D-FEM simulation result for a heater length of $80\mu m$ is shown in Fig. 7. It is assumed that $T_e(z)$ is the temperature profile for each layer and $n(z)$ is the new refractive index for each layer at temperature $T_e(z)$. By using n(z) as the input parameters for an optical mode solver, new effective refractive indices $n_e(z)$ along the propagation direction can be determined. As a result, the phase shift originating from the thermo-optic effect can be expressed by

$$\Delta\varphi = \frac{2\pi}{\lambda}\int_{-\infty}^{+\infty} n_e(z)dz \tag{5}$$

Next, in order to evaluate the speed of the device, a transient analysis is considered. Figures 8(a) and 8(b) present the change of the waveguide core temperature with time for the modified designs of Fig. 2 with the air trenches. The heater temperature is 425^0C.

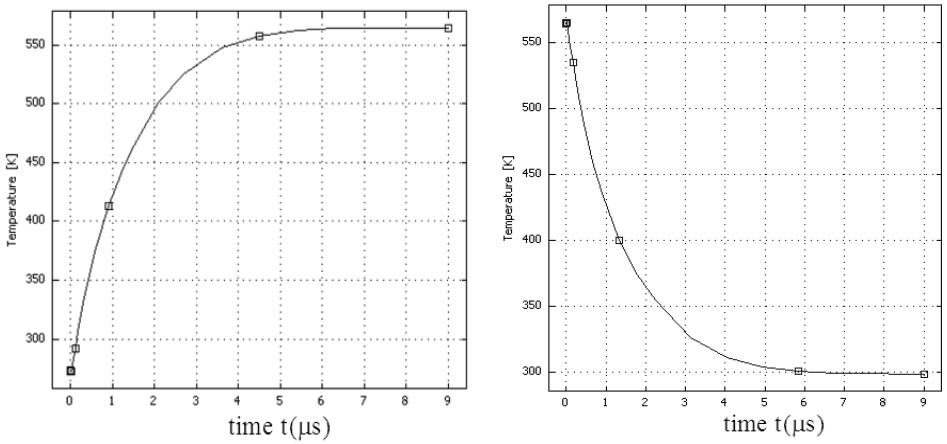

Figure 8. Time response (a) rise time response and (b) fall time response at the centre of the waveguide core for the modified design with the air trenches. The heater temperature is 425^0C (698 K)

The time response for heating $f_r(t)$ and cooling $f_f(t)$ can be described in terms of exponential functions as follows

$$f_r(t) = T_0 + \Delta T[1 - \exp(-\frac{t}{\tau_r})] \tag{6}$$

and

$$f_f(t) = T_0 + \Delta T \exp(-\frac{t}{\tau_f}) \tag{7}$$

where $T_0 = 25^0 C$, $\Delta T = T_{max} - T_0$ and T_{max} is the maximum temperature of the core waveguide. In this case, $T_{max} = 269\ ^0C$ (or 567 K) . Here, τ_r and τ_f are the time constants for heating and cooling, respectively.

The 10% - 90% rise time t_r is given by

$$t_r = 2.2\tau_r \tag{8}$$

and the 10% - 90% fall time t_f is given by

$$t_f = 2.2\tau_f . \tag{9}$$

Fitting the exponential functions of equations (6) and (7) to the calculated time responses shown in Fig. 8(a) and 8(b) gives the following table.

Table 1. Thermo-physical simulation for SOI waveguide structures

Structure	$\tau_r\,(\mu s)$	$\tau_f\,(\mu s)$	$t_r\,(\mu s)$	$t_f\,(\mu s)$	$t_a\,(\mu s)$	$f_c = \frac{0.35}{2t_a}$
Fig. 1(a)	3.90	2.90	8.58	6.38	8.58	20 kHz
Fig. 1(b)	2.04	1.6	4.49	3.52	4.49	39 kHz
Fig. 2	1.42	1.14	3.12	2.5	3.12	56 kHz

It can be seen from Table 1 that the modified waveguide structure has a cut-off frequency f_c more than twice that of the conventional structure of Fig. 1(b) and more than three times that of the conventional structure of Fig. 1(a).

In general, the modified designs can be applied to any device based on the thermo-optic effect in the SOI platform. In addition, the method presented in this subsection has shown to be a useful method for designing variable devices based on the thermo-optic effect. The modified design for the thermo-optic waveguides limits the heat flow to the desired locations in order to maximize the speed while minimizing power consumption.

4. CONCLUSIONS

In this paper, a new design for thermo-optic waveguides on the SOI platform has been presented. The new design has advantages of high speed and low consumption power compared to the conventional designs. The designs for these waveguides were optimized using the FEM method. In addition, a method for calculating accurately the phase shift induced by the thermo-optic effect was presented.

REFERENCES

1. L. Cahill and T. T. Le - The design of signal processing devices employing SOI MMI couplers, Integrated optoelectronic devices (OPTO 2009), Photonics West, Proceedings of the SPIE, San Jose Convention Center, San Jose, California, USA, 24 - 29 January 2009.
2. B. R. Koch, A. W. Fang, O. Cohen, and J. E. Bowers - Mode-locked silicon evanescent lasers, Optics Express **15** (2007) 11225-11233.
3. L. Liao, D. Samara-Rubio, and M. M. e. al. - High speed silicon Mach-Zehnder modulator, Optics Express **13** (2005) 3119-2135.
4. M. Harjanne, M. Kapulainen, T. Aalto, and P. Heimala - Sub-μs switching time in silicon-on-insulator Mach–Zehnder thermooptic switch, IEEE Photonics Technology Letters **16** (2004) 2039-2041.
5. T. T. Le - Design and analysis of optical filters using 3x3 multimode interference couplers based microring resonators, Journal of Sciences and Technology, Vietnam Academy of Sciences **46** (2) (2008) 39-48.
6. M. J. Weber - Handbook of Optical Materials: CRC, 2002.
7. H. S. Carslaw, H. S. Carslaw, and J. C. Jaeger - Conduction of Heat in Solids: Oxford University Press, 1986.

TÓM TẮT

THIẾT KẾ TỐI ƯU CẤU TRÚC ỐNG DẪN SÓNG QUANG TÍCH HỢP SỬ DỤNG HIỆU ỨNG QUANG-NHIỆT TRÊN CÔNG NGHỆ SILICON

Bài báo trình bày phương pháp thiết kế tối ưu cấu trúc ống dẫn sóng quang sử dụng hiệu ứng quang nhiệt trên công nghệ silicon (SOI). Để tính toán chính xác các tham số tốc độ (chuyển mạch) và phân bố nhiệt độ…, phương trình truyền nhiệt trong cấu trúc thiết bị được giải bằng phương pháp FEM. Bài báo cũng chỉ ra các ưu điểm của cấu trúc được đưa ra so với cấu trúc truyền thống khác. Đồng thời, lần đầu tiên, một công thức tính chính xác độ dịch pha do hiệu ứng quang- nhiệt trong ống dẫn sóng được đề xuất.

Từ khóa. Ống dẫn sóng quang, hiệu ứng quang- nhiệt, SOI.

Địa chỉ:

Department of Electronic Engineering,

La Trobe University, Australia.

Nhận bài ngày 25 tháng 7 năm 2009